III.3 Hydrogen Embrittlement of Pipelines: Fundamentals, Experiments, Modeling

P. Sofronis (Primary Contact), I.M. Robertson, D.D. Johnson
University of Illinois at Urbana-Champaign
Department of Materials Science and Engineering
1304 West Green Street
Urbana, IL 61801
Phone: (217) 333-2636; Fax: (217) 244-6534
E-mail: sofronis@uiuc.edu

DOE Technology Development Manager: Monterey R. Gardiner
Phone: (202) 586-1758; Fax: (202) 586-9811
E-mail: Monterey.Gardiner@ee.doe.gov

DOE Project Officer: Paul Bakke
Phone: (303) 275-4916; Fax: (303) 275-4753
E-mail: Paul.Bakke@go.doe.gov

Contract Number: GO15045

Start Date: May 1, 2005
Projected End Date: March, 31, 2010

Objectives

- Mechanistic understanding of hydrogen embrittlement in pipeline steels in order to devise fracture criteria for safe and reliable pipeline operation under hydrogen pressures of at least 15 MPa and loading conditions both static and cyclic (due to in-line compressors).
- Explore methods of mitigation of hydrogen-induced failures through inhibiting species (e.g., water vapor) or regenerative coatings (e.g., surface oxidation).
- Explore suitable steel microstructures to provide safe and reliable hydrogen transport at reduced capital cost.
- Assess hydrogen compatibility of the existing natural gas pipeline system for transporting hydrogen.

Technical Barriers

This project addresses the following technical barriers from the 3.2.4 Technical Challenges Section of the DOE Hydrogen, Fuel Cells, and Infrastructure Technologies Multi-Year Research, Development and Demonstration Plan:

(D) High Capital Cost and Hydrogen Embrittlement of Pipelines

(G) Storage Tank Materials and Costs

(J) Other Refueling Site/Terminal Operations

(K) Safety, Codes and Standards, Permitting

Technical Targets

This project is conducting fundamental studies of hydrogen embrittlement of materials using both numerical simulations and experimental observations of the degradation mechanisms. Based on the understanding of the degradation mechanisms, the project's goal is to assess the reliability of the existing natural gas pipeline infrastructure when used for hydrogen transport, suggest possible new hydrogen-compatible material microstructures for hydrogen delivery, and propose technologies (e.g. regenerative coatings) to remediate hydrogen-induced degradation. These studies meet the following DOE technical Targets for Hydrogen Delivery as mentioned in Table 3.2.2 of the October 2007 edition of the Hydrogen, Fuel Cells, and Infrastructure Technologies Multi-Year Research, Development and Demonstration Plan:

- *Pipelines: Transmission*–Total capital investment will be optimized through pipeline engineering design that avoids conservatism. This requires the development of failure criteria to address the hydrogen effect on material degradation (2012 target).
- *Pipelines: Distribution*–Same cost optimization as above (2012 target).
- *Pipelines: Transmission and Distribution*– Reliability relative to H_2 embrittlement concerns and integrity. The project's goal is to develop fracture criteria with predictive capabilities against hydrogen-induced degradation (2017 target). It is emphasized that hydrogen pipelines currently in service operate in the absence of any design criteria against hydrogen-induced failure.
- *Off-Board Gaseous Hydrogen Storage Tanks (Tank Cost and Volumetric Capacity)*–Same cost optimization as in *Pipelines: Transmission* above. Current pressure vessel design criteria are overly conservative by applying conservative safety factors on the applied stress to address subcritical cracking. Design criteria addressing the hydrogen effect on material safety and reliability will allow for higher storage pressures to be considered (2010 target).

Accomplishments

- Characterized the microstructure of pipelines steels through optical analysis, scanning electron

microscopy (SEM), and transmission electron microscopy (TEM); and identified particle composition through energy dispersive spectroscopy (EDS) for: a) laboratory specimens from Air Liquide and Air Products industrial pipelines; b) new microalloyed, low-carbon steels provided by DGS Metallurgical Solutions, Inc.

- Measured the macroscopic flow characteristics of the new microalloyed, low-carbon steels, possibly hydrogen compatible.
- Designed and validated a hydrogen permeation device for hydrogen permeability measurements.
- Developed, tested, and validated a finite element code for the study of transient stress-driven hydrogen transport coupled with large strain material elastoplastic deformation. The code has been used to simulate hydrogen uptake through the crack tip of an axial crack along the pipeline inner diameter (ID) surface.
- Determined the intensity of the hydrostatic constraint ahead of an axial crack on the ID surface. Laboratory specimen type (hydrostatic constraint guidelines) has been identified to investigate fracture conditions in a real-life pipeline.
- Characterized quantitatively through ab initio calculations the hydrogen effect on grain boundary cohesion in body-centered cubic (BCC) iron.

Introduction

Hydrogen is a ubiquitous element that enters materials from many different sources. It almost always has a deleterious effect on material properties. The goal of this project is to develop and verify a lifetime prediction methodology for failure of materials used in pipeline systems and welds exposed to high-pressure gaseous environments. Development and validation of such predictive capability and strategies to avoid material degradation is of paramount importance to the rapid assessment of the suitability of using the current pipeline distribution system for hydrogen transport and of the susceptibility of new alloys tailored for use in hydrogen related applications.

Through our hydrogen permeation rig, we measured the permeability of steel samples from industrial pipelines (Air Liquide and Air Products) and some new possibly hydrogen-compatible microalloyed, low-carbon steels. We used electron microscopy techniques to characterize the microstructure of these steels. Such characterization is important for the identification of the hydrogen trapping states in the material. We carried out finite element calculations of transient hydrogen transport simulating hydrogen uptake and transport through an axial crack on the ID surface of a pipeline. We demonstrated that small-scale yielding conditions are appropriate to analyze crack tip response for hydrogen pressures as high as 15.0 MPa and that constraint fracture mechanics is a promising approach toward avoiding conservatism in the design of the pipelines. We determined through first-principles calculations that hydrogen can reduce the internal cohesion of grain boundaries in iron by as much as 15%. Such assessment of internal material cohesion helps to construct interfacial cohesive models that are used in finite element simulation of hydrogen-induced fractures in laboratory specimens.

Approach

Our approach integrates mechanical property testing at the microscale, microstructural analyses and TEM observations of the deformation processes of materials at the micro- and nano-scale, first principle calculations of interfacial cohesion at the atomic scale, and finite element modeling and simulation at the micro- and macro-level.

In order to come up with fracture criteria for safe pipeline operation under hydrogen pressures of at least 15.0 MPa we investigate the interaction of hydrogen transient transport kinetics with material elastoplastic deformation ahead of an axial crack either on the ID or the outer diameter (OD) surface of a pipeline. Understanding of this interaction requires the determination of the elastic and flow characteristics of pipeline materials in the presence of hydrogen, and the measurement of the hydrogen adsorption, permeability, and bulk diffusion characteristics, such as the nature and strength of microstructural trapping sites for hydrogen. These experimental data are used in finite element simulations of the hydrogen distribution ahead of a crack tip in an effort to understand the transient and steady-state hydrogen population profiles. These profiles in conjunction with information from static fracture toughness, fatigue, and subcritical crack growth experiments will help to establish the regime of critical hydrogen concentrations and critical elapsed time for a crack to remain stable under high hydrogen pressure.

To quantitatively describe the hydrogen effect on internal material cohesion as a function of the hydrogen concentration under transient hydrogen conditions, we devised a thermodynamic theory of decohesion at internal material interfaces such as grain boundaries, precipitate/matrix, and second-phase/matrix interfaces. First-principles calculations of the hydrogen effect on these interfaces, which constitute potential fracture initiation sites, are used to calibrate the parameters of the thermodynamic theory such as the ratio of the reversible work of separation in the presence of hydrogen to that in the absence of hydrogen. The first-principles calculation results and the thermodynamics-based description of material cohesion

provide hydrogen-dependent traction-separation laws. These laws in conjunction with the finite element determination of the hydrogen concentration profiles ahead of a crack tip allow for the simulation of hydrogen-induced fracture and in turn for the development of engineering fracture criteria in terms of macroscopic parameters.

Results

Permeation measurements

A hydrogen permeation rig has been built (see Figure 1 of last year's progress report) and validated. Currently, the system is used to carry out permeation measurements as a function of temperature and hydrogen pressure. The materials tested are steels provided by DGS Metallurgical Solutions Inc and sample specimens taken from hydrogen pipelines operated by Air Liquide and Air Products. One of these steel samples–designated as type Steel C in last year's progress report–is a typical low carbon (0.04% by wt.) Mn-Si-single microralloy API/Grade X70/X80 capable of producing a ferrite/acicular microstructure. Permeability results for steel type C are shown in Figure 1. Figure 1a shows the normalized flux J/J_∞ as a function of permeation time till conditions of steady-state hydrogen diffusion through the permeation membrane are established. It has been determined that it typically takes two permeation transients to fully saturate the traps and all samples are tested three times (Figure 1b), with the third flux-transient being the one used in the analysis (Figure 1a). The product of the steady-state flux J_∞ with the membrane thickness L is plotted against the square root of the hydrogen pressure at room temperature (Figure 1c). The slope of this curve which is equal to 1.9×10^{12} H atoms/($\sqrt{\text{MPa}}$ m s) is the hydrogen permeability Φ through the material. Figure 1d shows the Arrhenius relationship of the permeability with temperature. As can be seen, the permeability data from measurements at Illinois and the Oak Ridge National Laboratory (ORNL) furnish an activation energy of 66.6 kJ/mol. The data from ORNL were taken at higher pressure and temperature than at

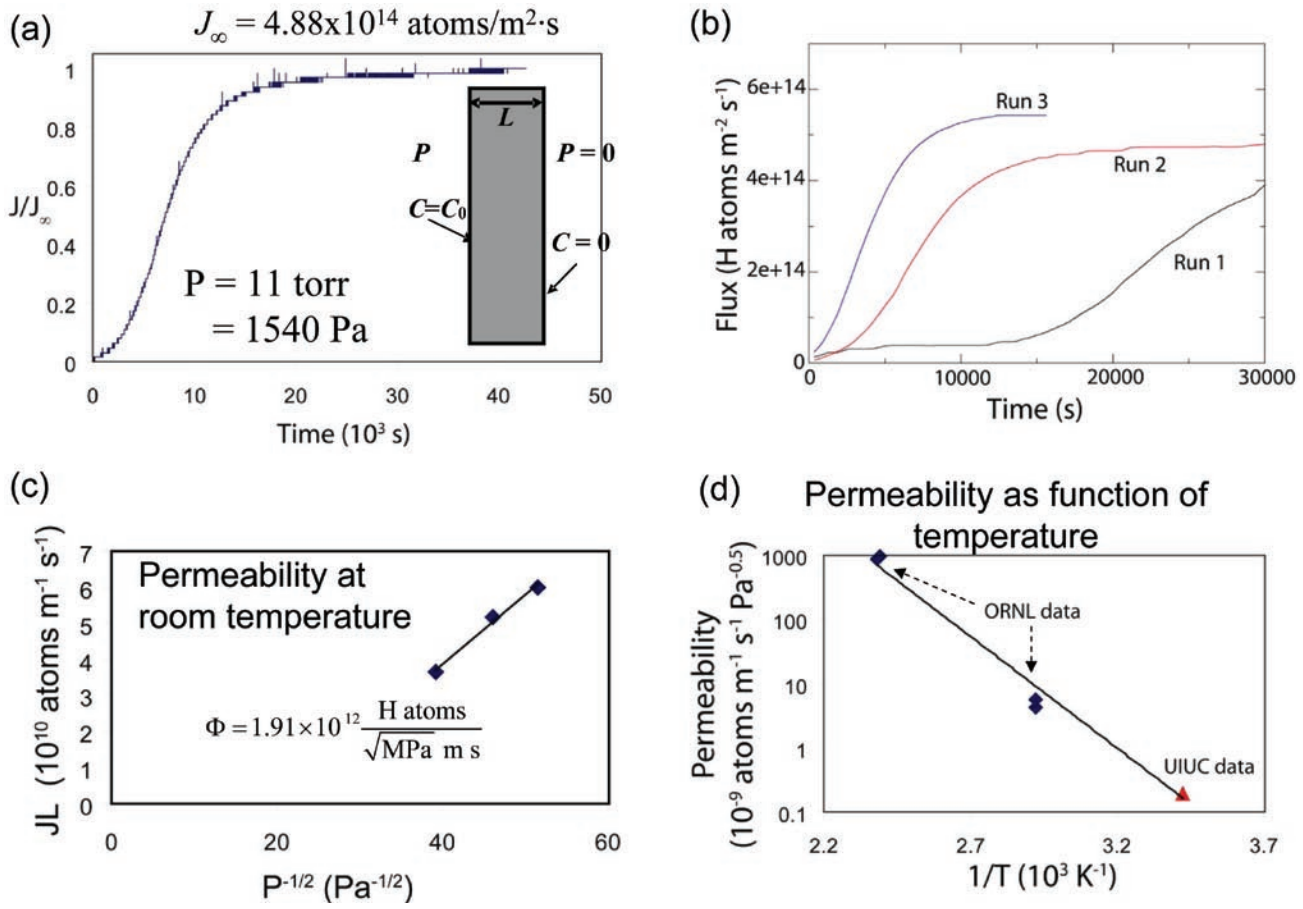

FIGURE 1. Hydrogen permeation: (a) Plot of normalized hydrogen flux J/J_∞ vs. time through a steel membrane of thickness $L = 120$ μm. The parameter J_∞ is the steady state flux measured in hydrogen atoms per square meter per second; (b) Third permeation transient is required for trap saturation; (c) Plot of the product $J_\infty L$ against the square root of pressure for the calculation of permeability Φ; (d) Plot of permeability as a function of temperature for the calculation of the activation energy.

Illinois. The confirmation of the Arrhenius relationship through data from the two laboratories verifies the independence of the relationship from the system used and hence the accuracy of the Illinois measurements.

The integral over time of the steady-state hydrogen flux J_∞ through the membrane when plotted as a function of time provides the time lag $t_T = L^2/6D_{eff}$ which represents the time required for hydrogen to diffuse through the membrane under steady-state conditions, that is, after the trapping microstructural defects have been filled out by hydrogen. The parameter $D_{eff} = D/(1+\partial C_T/\partial C_L)$ denotes the effective diffusion coefficient which accounts for trapping, D is the lattice diffusion constant, and C_L and C_T are respectively the lattice and trapping site concentrations. It is noted that in the absence of trapping the time lag is given by $t_L = L^2/6D$. From the measured time lag values t_T one calculates the effective diffusion coefficient D_{eff}. Matching the calculated values of the effective diffusion coefficient with corresponding finite element simulation predictions yields the lattice diffusion coefficient D as a function of temperature. These studies are currently under way.

The design of the permeation experimental apparatus and the related hydrogen permeation measurements meet all objectives of the project.

Microstructural Characterization

All materials (steel samples designated by A, B, and C) provided by DGS Metallurgical Solutions, Inc. and sample specimens taken from hydrogen pipelines operated by Air Liquide have been completely characterized.

In type C steel, particles and high dislocation densities are observed along with irregular grain boundaries, indicative of a microstructure that has not been fully recrystallized and recovered. Figure 2a shows results from EDS performed on a C sample. The fine particles inside the ferrite grains have been identified as precipitates composed of Ti and Nb. Optical analysis shows a grain size of 35 μm with 3% by volume pearlite grains (Figure 2b). SEM has shown the presence of larger sulfide and oxide particles typically containing Al and Mg (Figure 2c). The type B steel microstructure has very similar features. The grain size is slightly finer (30 μm) and the pearlite is 4%. Fine particles (100 μm) containing Ti and Nb were identified through TEM and EDS. SEM shows large (1 μm) Al and Mn rich sulfides. The type A steel has slightly larger grains (40 μm), as is expected with the lowest amount of Nb and 5% pearlite. Large Al rich sulfides were found with SEM and EDS.

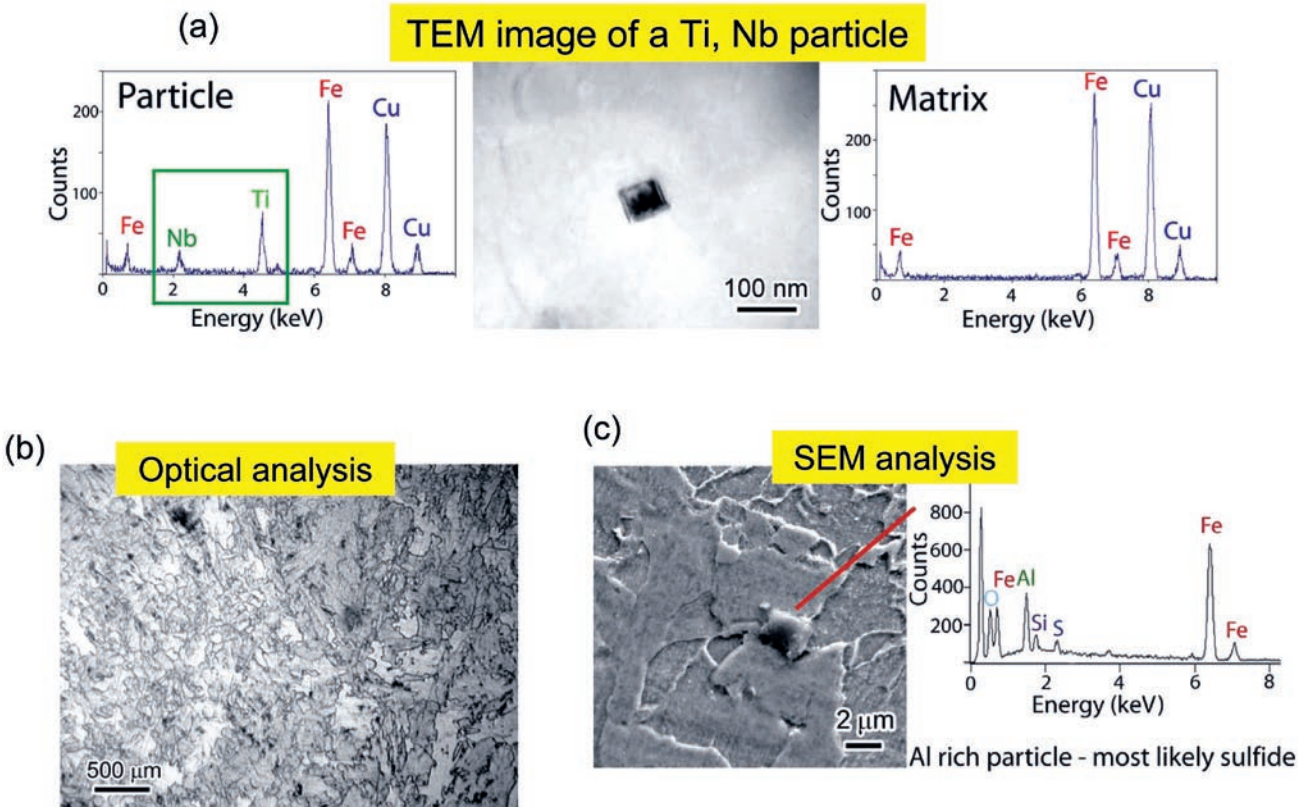

FIGURE 2. Microstructural Characterization of the C-type Steel (DGS Metallurgical Solutions, Inc)

Air Liquide steel samples show a much larger amount of pearlite (20%) than the steel samples A, B, and C, and smaller grain size (5 μm). In addition, isolated large (500 nm) cementite particles were found and were typically intergranular. Small (100 nm) Nb rich carbides are also present. SEM showed a low density of Al and Mn rich sulfides.

Micro- and Macro-Modeling and Simulation

Finite element calculations of transient hydrogen transport have been carried under plane strain conditions to simulate hydrogen uptake and transport in the neighborhood ahead of an axial crack on the ID surface of a pipeline carrying hydrogen at 15 MPa. The analysis was performed over the cross sectional domain of a typical pipeline geometry with OD equal to 40.64 cm (16") and wall thickness $h = 9.52$ mm (0.375").

The simulations model transient hydrogen transport driven by hydrostatic stress and account for trapping of hydrogen at microstructural defects (dislocations) whose density increases with plastic straining. Hydrogen resides either at normal interstitial lattice sites (NILS) or reversible trapping sites at microstructural defects generated by plastic deformation with corresponding concentrations C_L and C_T. The two populations are in equilibrium according to Oriani's theory. The governing equation for transient hydrogen diffusion accounting for trapping and hydrostatic-stress drift can be found in the work by Liang and Sofronis [1] and Dadfarnia *et al.* [2]. The interstitial hydrogen expands the lattice isotropically and its partial molar volume in solution is 2.0 x 10^{-6} m^3/mole. The problem of simulating material deformation and local hydrogen distributions is coupled in a non-linear sense and the solution procedure involves iteration [1]. In the calculations, the hydrogen diffusion coefficient through NILS at 300 K was assumed to be 2 x 10^{-11} m^2/s. We note that the assumed diffusion value reflects the nature of the ferritic microstructure in pipeline steels. The trap density was assumed to increase with plastic straining according to the experimental results of Kumnick and Johnson [3] and the trap binding energy was 60 kj/mole. The trap characteristics and the diffusion coefficient will be re-considered following the completed microstructural characterization and the permeation measurements we plan in the experimental component of our project.

Tabata and Birnbaum [4] observed that the local flow stress in iron decreases with hydrogen concentration. Following Sofronis *et al.* [5], we consider that the flow stress of the material decreases linearly with the amount of hydrogen trapped at dislocations: $\sigma_Y(\varepsilon^p, C_T) = \sigma_0^H(C_T)(1+\varepsilon^p/\varepsilon_0)^n$, where $\sigma_0^H(C_T) = \sigma_0[1+(\xi-1)C_T/C_r]$ is the yield stress in the presence of hydrogen, σ_0 and ε_0 are respectively the yield stress and strain in the absence of hydrogen, ε^P is the logarithmic strain in uniaxial tension, n is the hardening exponent, $\xi \le 1$ is a parameter describing the extent of softening, and C_r is a reference concentration. The numerical simulations were carried out for the C type steel whose material properties are reported in the 2006 annual progress report. On the crack faces and the ID surface that were loaded by the hydrogen pressure a concentration $C_0 = 2.659$ x 10^{22} H atoms/m^3 (= 3.142 x 10^{-7} H atoms per solvent atoms) in equilibrium with the gas pressure was prescribed. We assumed $\xi = 0.96$ for the softening parameter and $C_r = C_0$. The OD surface of the pipe was assigned a zero concentration boundary condition.

The solutions for the hydrostatic stress and steady state hydrogen concentrations at NILS ahead of the crack tip for crack depths $a = 0.476$ mm ($a/h = 0.05$) and $a = 1.9$ mm ($a/h = 0.2$) are plotted in Figure 3. The stress intensity factor K_I and the T-stress for each crack depth are also reported. The T-stress is the second, non-singular constant term in the asymptotic mode I linear elastic crack-tip field and represents a stress acting parallel to the crack plane (Figure 3). The hydrostatic stress profiles ahead of the crack tip are coincident for both crack sizes. As a result, the associated peak values of the hydrogen concentration are also the same. The simulations show that for $a/h < 0.4$ the near tip profiles of the hydrostatic stress and steady-state normalized hydrogen concentration at NILS are independent of the crack depth. We also found [2] that the profiles for the stress and deformation fields and those for the steady-state hydrogen concentration near the tip of the axial pipeline crack are the same as those calculated through a modified boundary layer formulation [6] in terms of the stress intensity factor and the T-stress the actual crack in the pipeline experiences. In addition,

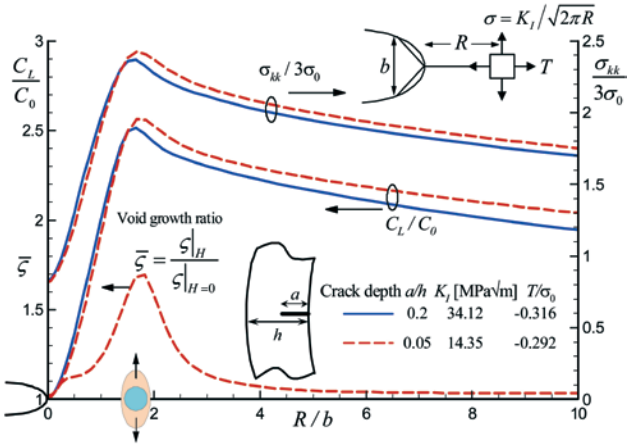

FIGURE 3. Comparison of the hydrostatic stress $\sigma_{kk}/3\sigma_0$ and steady state normalized NILS hydrogen concentration C_L/C_0 at the tip of an axial crack on the ID surface of a pipeline for two different crack depths. The parameter $\sigma_0 = 595$ MPa is the yield stress of the material and $C_0 = 2.659 \times 10^{22}$ H atoms/m^3 denotes the NILS hydrogen concentration in equilibrium with hydrogen gas at pressure 15 MPa. The small-scale character of the solutions renders the profiles independent of the crack depth.

we found that the near tip results in the boundary layer formulation are independent of the size of the domain of analysis [2]. Therefore, conditions for hydrogen-induced fracture at a pipeline axial-crack can be studied with laboratory fracture mechanics specimens in which the crack tip hydrostatic constraint is the same as that in front of the crack in the pipeline. This result allows for the exploration of a J_{IC}-T fracture locus approach, where J_{IC} is the material fracture toughness. It is worth noting that such a constraint-based fracture mechanics approach eliminates the conservatism embedded in the design against fracture based on J_{IC} alone.

The role of hydrogen on void growth ahead of the axial crack was quantified by employing the model of Rice and Tracey [7]. The effect was assessed through the normalized void-growth parameter $\bar{\zeta} = \zeta / (\zeta|_{\xi=1})$ denoting the ratio of a void-growth parameter ζ in the presence of softening to that in the absence of hydrogen [2]. The parameter $\bar{\zeta}$ is plotted in Figure 3. Clearly, hydrogen-induced softening accelerates void growth ($\bar{\zeta}>1$) in the fracture process zone ($R/b<3$), with the rate of growth becoming larger at the hydrostatic stress peak location. The parameter b denotes the crack opening displacement which is a function of the applied stress intensity factor.

The simulations described in this section are essential prerequisites toward meeting all objectives of our project.

First-Principles Assessment of Hydrogen Effects on Interfacial Cohesion

Ab initio density-functional-theory (DFT) calculations can reveal directly the key bonding and surface-energy effects (grain boundary, free surface, or interphase boundaries) that control interfacial cohesion in the presence of hydrogen solute atoms.

We have completed validation "computer experiments" on the binding energies for H in Fe $\Sigma3[1\bar{1}0](111)$ grain boundary and free surface using a plane-wave pseudopotential method with projected-augmented wave basis, as implemented in the Vienna ab initio Simulation Package (VASP). A subset of our validation results provides (un)relaxed binding energies for H in Fe for grain boundary/free surface for various values of hydrogen coverage, from 0 to 100%. Figures 4a and 4b show the difference in charge densities at the BCC Fe $\Sigma3[1\bar{1}0](111)$ grain boundary and free surface, respectively, which is calculated by taking the H/Fe charge density and subtracting the charge density obtained by superimposing atomic H and the hydrogen-free Fe grain boundary (Figure 4a)/ free surface (Figure 4b) at the same atomic position of the true H/Fe system. Clearly, Figure 4a shows that electrons are removed from Fe atoms adjacent to the grain boundary and transferred to Fe atoms within the grain boundary, leading to decohesion as fewer electrons participate in the Fe-Fe bonds that straddle the grain boundary (loss of bonding).

We calculated the hydrogen-induced changes $\Delta(2\gamma_s)$ and $\Delta\gamma_{gb}$ to the surface and grain boundary energies, respectively, and determined the reversible work of decohesion $(2\gamma_{int})_{\theta_{int}}$ at grain boundary coverage θ_{int} in terms of the reversible work $(2\gamma_{int})_0$ in the absence of hydrogen. It is commonly assumed incorrectly that the hydrogen-induced change to the reversible work of separation $\Delta E = (2\gamma_{int})_{\theta_{int}} - (2\gamma_{int})_0 = \Delta(2\gamma_s) - \Delta\gamma_{gb}$ varies linearly with hydrogen coverage. However, the linear approximation is a ~20% low estimate due to the larger effect the hydrogen has on decohesion within the grain boundary of Fe at high values of coverage. Figure 4c shows that without relaxation there is a clear linear behavior, whereas there is actually an increased embrittlement effect due to the internal relaxations related to charge-density rearrangements shown in Figures 4a and 4b.

These results are used to calibrate the parameter $k = (2\gamma_{int})_{\theta_{int}=1}/(2\gamma_{int})_0$ of the traction-separation law $\sigma(\theta_{int}, q) = 27\sigma_{max}[1 + (k-1)\theta_{int}]q(1-q)^2/4$ as furnished by the thermodynamic theory of interfacial decohesion of Mishin et al. [8], where q is separation normalized by the maximum separation upon decohesion and σ_{max} is the cohesive stress in the absence of hydrogen. This law is currently used in finite element simulations of hydrogen-induced grain boundary decohesion.

These first-principles calculations are required to establish fracture criteria accounting for the hydrogen effect (all project objectives).

Conclusions and Future Directions

- A finite element simulation code for transient hydrogen transport analysis ahead of a crack tip on the ID and OD surfaces of a pipeline has been developed and tested. The code can treat stress-driven diffusion through interstitial lattice sites and trapping of hydrogen at microstructural defects.
- Hydrogen transport simulations have been carried in which material deformation is coupled with hydrogen-induced degradation in the form of hydrogen-accelerated void growth.
- We demonstrated that the deformation conditions ahead of a crack tip in a pipeline can be described by a modified boundary layer formulation using the T-stress approach to characterize the hydrostatic constraint. We emphasize that such a constraint-based fracture mechanics approach eliminates the conservatism embedded in the design against fracture based on J_{IC} alone.
- A permeation measurement apparatus has been built and tested. Identification of the diffusion characteristics (e.g. permeability, solubility, trap

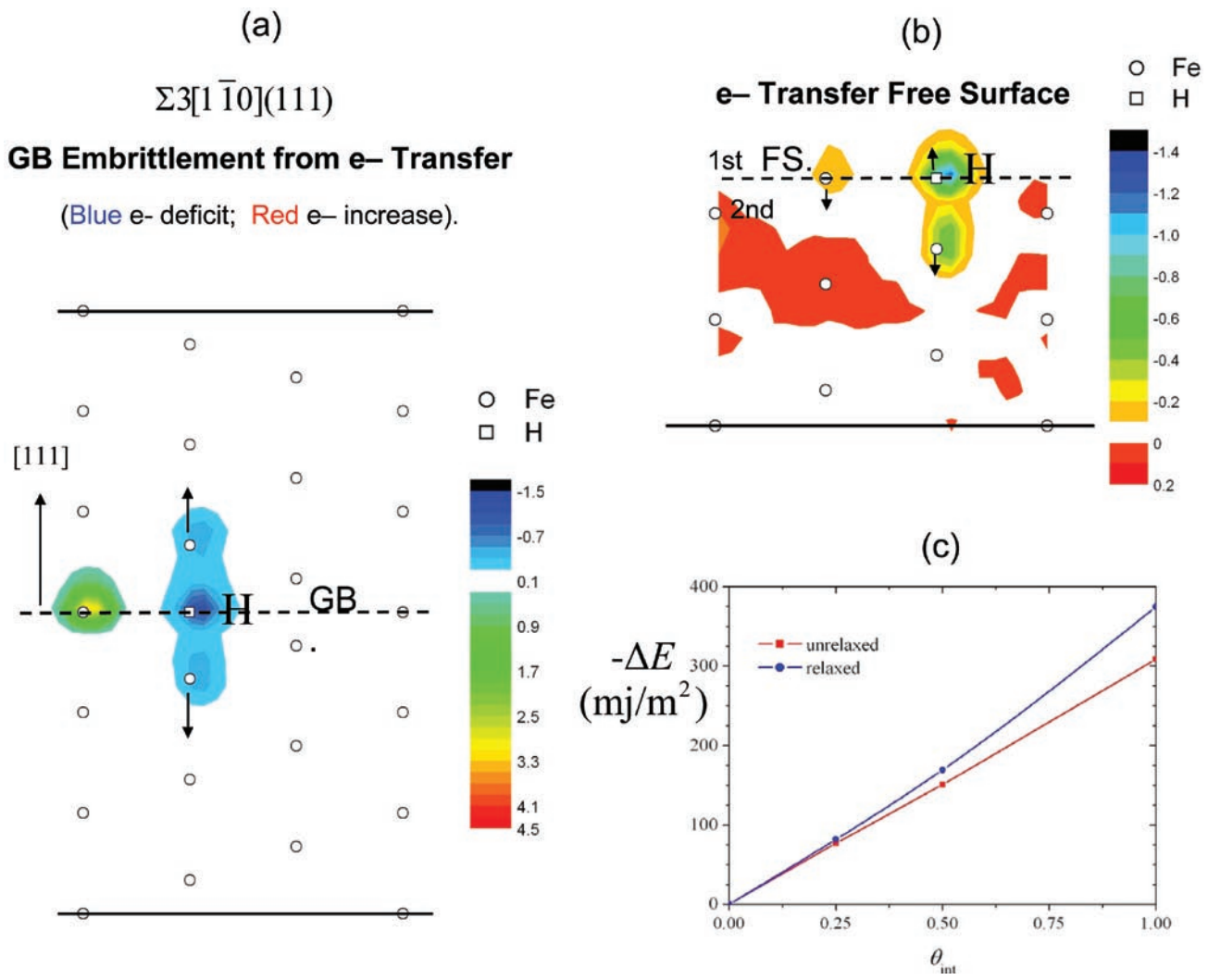

FIGURE 4. Electronic charge density difference contours for $\Sigma 3[1\bar{1}0](111)$ grain boundary (a) and free surface (b) in BCC Fe. Blue contours indicate electron deficit, while red contours electron enhancement. The difference is the total charge density of the H/Fe system minus the total density obtained by superimposing the density of atomic H and that of Fe at the same coordinates as the H/Fe systems. The loss of electrons from the two Fe atoms adjacent the grain boundary and H atom reduces the cohesion. For the free surface, charge is taken from the H atom at the surface and added to the second layer of Fe atoms; (c) Hydrogen-induced change ΔE in the reversible work of separation of the grain boundaries in BBC iron vs. hydrogen coverage θ_{int}.

strength and density) of existing and new pipeline steel microstructures is carried out with increasing membrane thickness to isolate and understand potential surface adsorption related effects.

- We completely characterized all materials provided by DGS Metallurgical Solutions, Inc. and sample specimens taken from hydrogen pipelines operated by Air Liquide.
- We used ab initio DFT calculations to determine the cohesive strength of material interfaces. We calculated that hydrogen can reduce the internal cohesion of grain boundaries in BCC iron by as much as 15%. Presently we are performing similar calculations to estimate fracture energies as a function of hydrogen coverage at various particle/matrix interfaces, such as Fe_3C/alpha-Fe and MnS/alpha-Fe interfaces.
- We will employ ab initio calculation results to calibrate thermodynamic models of interfacial decohesion needed for finite element simulations of the hydrogen effect at the macroscale.
- We will carry out fracture toughness testing along with SEM and TEM studies to identify the failure mechanisms and associated microstructural features in the presence of hydrogen.
- We continue our collaboration with the Hydrogen National Institute for Use and Storage (HYDROGENIUS) of Japan.

Special Recognitions & Awards/Patents Issued

1. P. Sofronis visited Japan from June 9 to June 25, 2006 as a fellow of the Japan Society for the Promotion of Science (JSPS) to collaborate on research related to hydrogen material compatibility.

2. P. Sofronis and I. Robertson were invited speakers at the *International Hydrogen Energy Development Fora* organized by HYDROGENIUS at Fukuoka, Japan on January 31 - February 1, 2007, and February 4-8, 2008.

FY 2008 Publications/Presentations

Publications

1. Dadfarnia, M., Somerday, B.P., Sofronis, P., Robertson, I.M., Stalheim, D. (In Print) Interaction of Hydrogen Transport and Material Elastoplasticity in Pipeline Steels, ASME *Journal of Pressure Vessel and Technology*.

2. Liang, Y., Ahn, D.C., Sofronis, P., Dodds, R. and Bammann, D. (2008) Effect of Hydrogen Trapping on Void Growth and Coalescence in Metals and Alloys, *Mechanics of Materials*, 40, 115-132.

3. Dadfarnia, M., Sofronis, P., Somerday, B.P., Robertson, I.M. (2008) On the small scale character of the stress and hydrogen concentration fields at the tip of an axial crack in steel pipeline: effect of hydrogen-induced softening on void growth, *International Journal of Materials Research (Formerly Z. Metallkd.)*, 99, 557-570.

4. Ahn, D. C., Sofronis, P. and Dodds, R. (2007) On Hydrogen-Induced Plastic Flow Localization During Void Growth and Coalescence, *International Journal of Hydrogen Energy*, 32, 3734-3742.

5. Dadfarnia, M., Somerday, B. P., Sofronis, P., Robertson, I.M. (In Print) Hydrogen/Plasticity Interactions at an Axial Crack in Pipeline Steel, *Journal of ASTM International (JAI)*.

6. Dadfarnia, M., Sofronis, P., Somerday, B.P., Robertson, I.M. (under review) Effect of remote hydrogen boundary conditions on the near crack-tip hydrogen concentration profiles in a cracked pipeline, *The American Ceramic Society's Ceramic Transactions Series*.

Presentations

1. Sofronis, P. (invited) "Hydrogen Embrittlement: Fundamentals, Modeling, and Experiment," Hydrogenenius Meeting on Materials Testing, Selection, and Standardazation, Japan-US members, Hotel Okura, Fukuoka, Japan, Nov. 8, 2007.

2. Dadfarnia, M., Somerday, B. P., Sofronis, P., Robertson, I.M. (contributed) "Hydrogen/Plasticity Interactions at an Axial Crack in Pipeline Steel," 36th ASTM National Symposium on Fatigue and Fracture Mechanics, Tampa, Florida, Nov. 14-16, 2007.

3. Sofronis P. (invited) "Hydrogen Embrittlement: A Case Study on the Transferability of Fracture Toughness Parameters between Laboratory Specimen and Real-life Structure," Los Alamos National Laboratory, New Mexico, January 10-11, 2008.

4. Sofronis, P. (invited) "Mechanics Models of Hydrogen Embrittlement for Steel Pipelines," Second International Hydrogen Energy Development Forum, Hotel Okura, Fukuoka, Japan, Feb. 6, 2008.

5. Ritchie, R.O. and P. Sofronis (invited) "Micromechanicms of Fracture: Role of Hydrogen Embrittlement," Second International Hydrogen Energy Development Forum, Hotel Okura, Fukuoka, Japan, Feb. 6, 2008.

6. Robertson, I. M. (invited) "Application of Controlled Environment Transmission Electron Microscope to Hydrogen Effects in Metals," Second International Hydrogen Energy Development Forum, Hotel Okura, Fukuoka, Japan, Feb. 6, 2008.

7. Sofronis P. (contributed) "Fracture Toughness Assessment of Hydrogen Pipelines," Symposium on Materials Innovations in an Emerging Hydrogen Economy. Organized by the American Ceramic Society, Cocoa Beach, Florida, February 25-27, 2008.

8. Sofronis, P. (invited) "Hydrogen Embrittlement: Fundamentals Experiments. Modeling," Department of Mechanical and Aerospace Engineering, Arizona State University, Tempe, AZ, April 18, 2008.

9. Sofronis, P. (invited) "A Combined Applied Mechanics/ Materials Science Approach Toward Understanding the Role of Hydrogen on Material Degradation in Low and High Strength Steels," ExxonMobil Research and Engineering Company, Annandale, New Jersey, April 23, 2008.

References

1. Liang, Y. and Sofronis, P. (2003) Toward a phenomenological description of hydrogen-induced decohesion at particle/matrix interfaces. *J. Mech. Phys. Solids*, 51, 1509-1531.

2. Dadfarnia, M., Sofronis, P., Somerday, B.P. and Robertson, I.M. (2008) On the small scale character of the stress and hydrogen concentration fields at the tip of an axial crack in steel pipeline: effect of hydrogen-induced softening on void growth. *Int. J. Mat Res.*, 99(5), 557-570.

3. Kumnick, A.J., and Johnson, H.H. (1980) Hydrogen transport through annealed and deformed iron. *Metall. Trans*, 1974, 5A, 1199-1206.

4. Tabata, T. and Birnbaum, H.K. (1983) Direct observations of the effect of hydrogen on the behavior of dislocations in iron. *Scr. Metall.*, 17(7), 947-950.

5. Sofronis, P., Liang, Y. and Aravas, N. (2001) Hydrogen induced shear localization of the plastic flow in metals and alloys. *Eur. J. Mech. A-Solid*, 20, 857-872.

6. Betegon, C. and Hancock, J.W. (1991) Two-Parameter Characterization of Elastic-Plastic Crack-Tip Fields," *Journal of Applied Mechanics*, 58, 104–110.

7. Rice, J.R. and Tracey, D.M. (1969) On the ductile enlargement of voids in triaxial stress fields, *J. Mech. Phys. Solids*, 17, 201-217.

8. Mishin, Y., Sofronis, P. and Bassani, J.L. (2002) Thermodynamic and kinetic aspects of interfacial decohesion, *Acta Materialia*, 50, 3609-3622.